JACS
JOURNAL OF THE AMERICAN CHEMICAL SOCIETY
pubs.acs.org/JACS
Article

Selective Glycan Labeling of Mannose-Containing Glycolipids in Mycobacteria

So Young Lee,[⊥] Victoria M. Marando,[⊥] Stephanie R. Smelyansky, Daria E. Kim, Phillip J. Calabretta, Theodore C. Warner, Bryan D. Bryson, and Laura L. Kiessling*

Cite This: J. Am. Chem. Soc. 2024, 146, 377−385

ABSTRACT: *Mycobacterium tuberculosis* (*Mtb*) is one of history's most successful human pathogens. By subverting typical immune responses, *Mtb* can persist within a host until conditions become favorable for growth and proliferation. Virulence factors that enable mycobacteria to modulate host immune systems include a suite of mannose-containing glycolipids: phosphatidylinositol mannosides, lipomannan, and lipoarabinomannan (LAM). Despite their importance, tools for their covalent capture, modification, and imaging are limited. Here, we describe a chemical biology strategy to detect and visualize these glycans. Our approach, biosynthetic incorporation, is to synthesize a lipid-glycan precursor that can be incorporated at a late-stage step in glycolipid biosynthesis. We previously demonstrated selective mycobacterial arabinan modification by biosynthetic incorporation using an exogenous donor. This report reveals that biosynthetic labeling is general and selective: it allows for cell surface mannose-containing glycolipid modification without nonspecific labeling of mannosylated glycoproteins. Specifically, we employed azido-(*Z*,*Z*)-farnesyl phosphoryl-*β*-D-mannose probes and took advantage of the strain-promoted azide−alkyne cycloaddition to label and directly visualize the localization and dynamics of mycobacterial mannose-containing glycolipids. Our studies highlight the generality and utility of biosynthetic incorporation as the probe structure directs the selective labeling of distinct glycans. The disclosed agents allowed for direct tracking of the target immunomodulatory glycolipid dynamics in cellulo. We anticipate that these probes will facilitate investigating the diverse biological roles of these glycans.

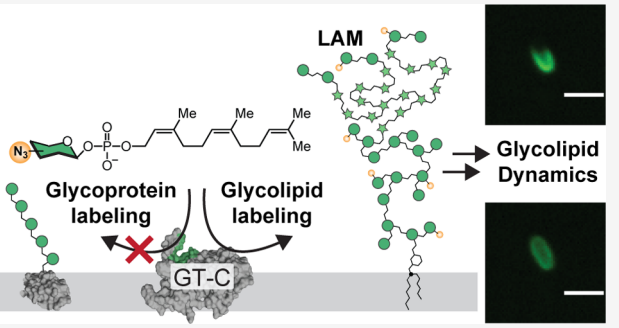

INTRODUCTION

Mycobacterium tuberculosis (*Mtb*) causes tuberculosis, which kills over one million people each year.[1] An estimated 3 billion people are infected with latent *Mtb* worldwide.[2] The ability of *Mtb* to suppress the host immune system during infection and persist in a latent form severely exacerbates its impact.[3−6] Mannose-containing glycolipids produced by mycobacteria, including phosphatidylinositol mannosides (PIMs), lipomannan (LM), lipoarabinomannan (LAM), and mannosylated lipoarabinomannan (ManLAM), modulate the host immune response.[7−12] Host recognition of bacterial glycans is critical for immune responses and pathogen clearance, and in the case of *Mtb*, mannose-containing glycolipids participate in multiple immune evasion mechanisms. For instance, LAM inhibits lysosome-phagosome fusion, allowing *Mtb* to form an intracellular niche within host macrophages.[13,14] Mannose-containing glycolipids have also been implicated in maintaining cellular integrity.[11,13]

Despite the importance of these glycolipids, few direct methods exist to study their biosynthesis, trafficking, and biological function. Monoclonal antibodies (mAbs) that recognize LAM or LM can be used,[15,16] yet an antibody's size (180 kDa) can limit its utility for visualizing the LAM (15 kDa) as structural occlusion of other membrane components can complicate in cellulo analyses.[17,18] Thus, new strategies are needed for the selective structural perturbation of mannose-containing glycans to probe their composition, function, and dynamics within the context of live cells and disease pathogenesis.[19]

Our understanding of the roles of these mannose derivatives would be enhanced by methods to visualize them. Because glycan biosynthesis is not directly genetically encoded, installing labels through genetic manipulation is difficult.[20] Metabolic incorporation offers an incisive route to installing handles into glycans.[21−25] The process involves multistep, intracellular processing of simple monosaccharide building blocks by endogenous metabolic machinery, culminating in the

Received: August 30, 2023
Revised: December 3, 2023
Accepted: December 5, 2023
Published: December 19, 2023

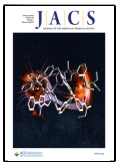

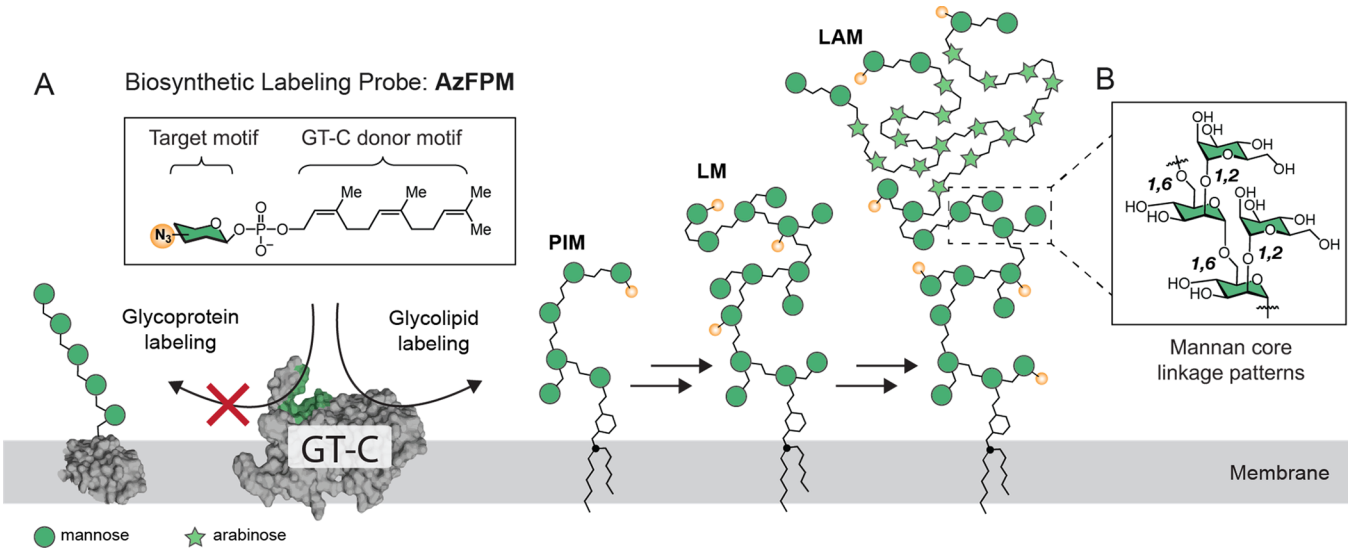

Figure 1. Overview schematic of biosynthetic labeling strategy targeting glycolipids. (A) Previous studies led to the identification of an effective lipid motif for membrane-associated glycosyltransferase recognition. We leverage this information to selectively label immunodulatory mycobacterial glycolipids with a novel suite of glycolipid probes (azido-(*Z*,*Z*)-farnesyl phosphoryl-*β*-D-mannose, AzFPM). (B) Mannose-containing glycolipids are elongated via 1,6-glycosidic bonds and feature branching at the 2-position.

presentation of the end products on the cell surface.[23] Though several successful examples have been demonstrated in bacteria, applying this strategy in these organisms poses challenges due to the complexity of glycan metabolism and catabolism in bacteria.[21,24,26−32]

The only known probe of the PIMs, LM, and LAM is based on the metabolic incorporation of azide-functionalized inositol.[33] Competition with the endogenous substrate occurs in multiple steps, so selective probe incorporation is contingent upon deleting genes in the endogenous inositol biosynthetic pathway. Though this requirement prevents the use of this probe in wild-type cells, these metabolic incorporation probes led to the discovery of a previously unidentified inositol transporter. Still, no probes for labeling cell-surface mannose residues have been disclosed.

Two key challenges render mannose an elusive target. First, mannose plays a central role in mycobacterial metabolism. The mannose precursors for the relevant mycobacterial glycans are generated from the isomerization of fructose-6-phosphate by mannose-6-phosphate isomerase or through mannose import and elaboration.[34,35] Intracellular mannose can be used for energy production or converted to fucose, rhamnose, or mannose sugar donors. Consequently, a probe that depends on metabolic incorporation would have a higher risk of off-target labeling than a probe that intervenes at a late-stage in biosynthesis. Second, glycolipid donor forms of mannose are used in mycobacteria for the biosynthesis of mannose-containing glycolipids and mannosylated proteins. Thus, distinguishing between these two classes of glycans via metabolic incorporation would be challenging. Such distinctions are important, however, as mannosylated proteins in mycobacteria are also linked to virulence.[7] Thus, dissecting the roles of different glycan structures depends on specific labeling strategies that differentiate between mannosylated glycoproteins and glycolipids.

We postulated that intervening late in the biosynthetic pathway could facilitate the labeling of the target structures with selectivity for glycolipids over glycoproteins. We define this late-stage metabolic engineering strategy as biosynthetic incorporation. To this end, we designed probes that could be used directly by glycosyltransferases, thereby limiting competition with endogenous substrates to a single step to increase labeling efficiency. Because most metabolic processes occur inside the cell, we postulated that agents that exploit extracellular enzymes would selectively modify specific cellular glycans such as glycolipids over glycoproteins. Neither the locale nor structure of the donor for protein mannosylation is well characterized in mycobacteria. However, the proposed dolichyl donor for glycoprotein biosynthesis and polyprenyl glycolipid donor structures vary in the degree of *β*−*γ* saturation, and preservation of this motif in farnesyl-bearing probes may enable specific modification of glycolipid targets.[36] Second, protein glycosylation is likely to occur intracellularly rather than at the cell surface, and thus, we hypothesized that selectivity could be dictated by probe localization and lack of uptake. This information gave us optimism that we could generate a selective probe of the mycobacterial glycolipids.

We previously synthesized and applied lipid-linked arabinofuranose derivatives that were incorporated into the mycobacterial cell envelope. Specifically, synthetic azido-(*Z*,*Z*)-farnesyl phosphoryl-*β*-D-arabinofuranose (AzFPA) derivatives function as surrogates for the endogenous arabinofuranose donor decaprenyl phosphoryl-*β*-D-arabinofuranose (DPA).[37,38] The shorter lipid facilitated exogenous reagent delivery such that the isomeric azide-substituted AzFPA probes led to an azide-containing arabinogalactan. We observed different modification levels depending on the bacterial species, and the data indicated that the azido-arabinose derivatives had been used by periplasmic glycosyltransferases to generate a modified arabinogalactan. LM and LAM synthesis also occurs in the periplasm mediated by the glycosyltransferase-C (GT-C) superfamily of mannosyltransferases that utilize a polyprenyl phosphoryl-*β*-D-mannose (PPM) as their donor.[39,40] Consequently, we leveraged this information to visualize and track these glycans.

Herein, we report the synthesis, validation, and application of probes to study mannose-containing glycolipids in model mycobacterial organisms and *Mtb* (Figure 1A). We prepared

https://doi.org/10.1021/jacs.3c09495
J. Am. Chem. Soc. 2024, 146, 377−385

Scheme 1. Design and Synthesis of AzFPM Probes[a]

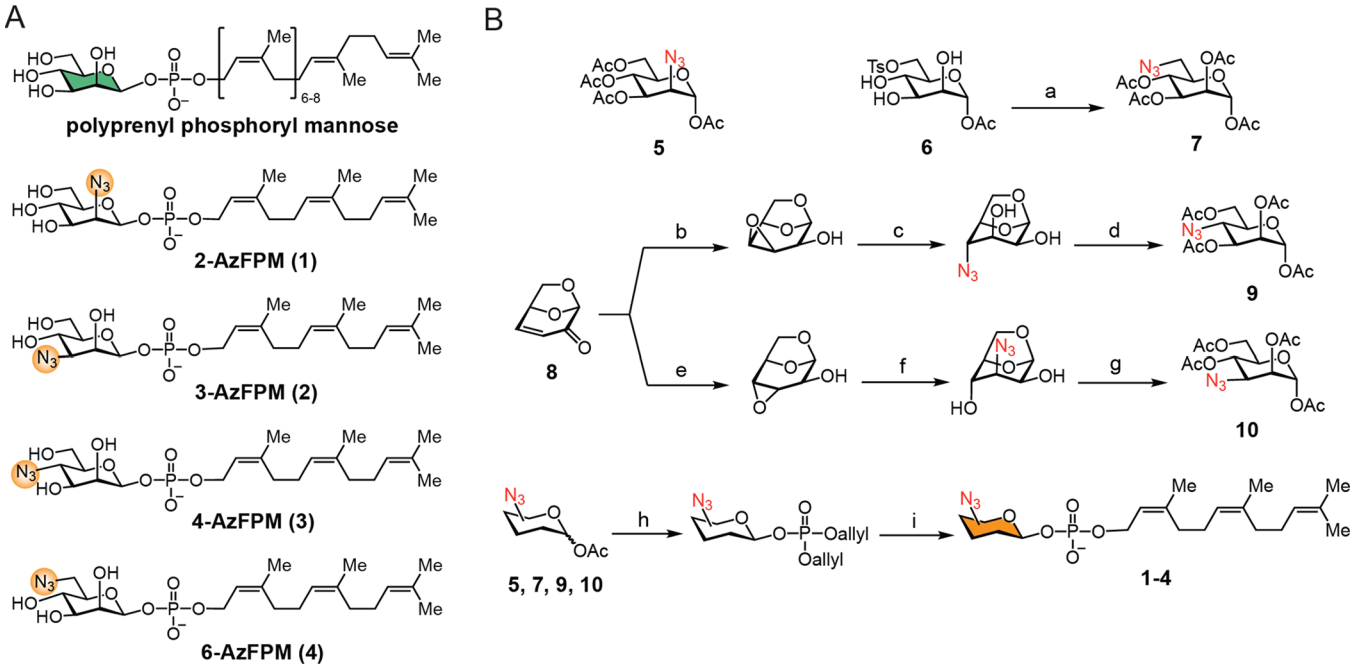

[a](A) Azide-modified substrate surrogates were designed based on structural homology to the endogenous mannose donor, polyprenyl phosphoryl mannose. Four azide regioisomers were produced (**1**−**4**). (B) Synthetic routes were established to produce **1**−**4**: a: (i) acetic anhydride, pyridine (78%), (ii) NaN_3, DMF (97%); b: (i) $NaBH_4$, $CeCl_3$ (93%), (ii) AgOAc, I_2, then MeOH, NH_4OH (88%); c: NaN_3, DMF (81%); d: TFA, acetic anhydride (84%, α:β = 1:0.36); e: (i) tBuOOH, DBU (58%), (ii) $NaBH_4$ (63%); f: NaN_3, DMF (69%); g: TFA, acetic anhydride (84%, α:β = 1:0.24); h: (i) NH_2NH_3OAc or benzylamine (68−88%), (ii) $POI(OAllyl)_2$ (46−68%); i: (i) $Pd(PPh_3)_4$, (ii) Cl_3CCN, (*Z*,*Z*)-farnesol, (iii) NH_3, MeOH (8−28% over three steps).

mannosylated lipid-linked donors with azide handles. These derivatives are successfully used by cells and, therefore, can be used to monitor specific glycans within the cell envelope. Our results underscore the generality of late-stage biosynthetic incorporation with a lipid-linked donor as a glycan bioconjugation strategy. Beyond demonstrating the generality, however, our findings highlight the specificity of this approach. We show the probes label mannosylated glycolipids over glycoproteins. Indeed, we could even selectively label subsets of glycolipids depending on the site of azide substitution. In validating the probes in *Mtb*, we provide new tools to study the roles of distinct glycans in disease.

RESULTS AND DISCUSSION

Design and Synthesis of Azido-Mannose Probes. Biosynthetic incorporation in mycobacteria has been applied to a single target, arabinose, within arabinogalactan.[37,41] We hypothesized that the approach would be general and could be exploited to differentiate between glycoprotein and glycolipid modification. Based on our previous success using a farnesyl motif to mimic the endogenous polyprenyl donor, we designed a panel of azido-(*Z*,*Z*)-farnesyl phosphoryl-β-D-mannose (AzFPM) derivatives (Scheme 1A). We generated this panel because we reasoned that the efficiency of non-natural mannose incorporation could vary between different isomers and between model species, as seen previously with arabinose derivatives.[37] Specifically, the core of the LAM is a polymer consisting of α-1,6 linked mannose residues, and this backbone is elaborated with 2-substituted α-mannose. This arrangement suggests that the incorporation of mannose derivatives with azido groups at 3 or 4 positions might be the least perturbing as they would not lead to chain truncation (Figure 1B). However, the efficiency of incorporation could be impacted by enzyme−substrate complementarity, so we also tested substrate mimics with azide groups at the 2 and 6 positions (Scheme 1A).

The site of azide group placement could also manifest in labeling differences between organisms as the LAM varies significantly. For instance, *Corynebacterium glutamicum* produces AraLAM, in which a mannan core is terminated with arabinose residues, whereas *Mycobacterium smegmatis* generates a phosphoinositol-capped PILAM, and *Mtb* affords a mannose-capped ManLAM. Accordingly, we prepared and evaluated all four possible regioisomeric AzFPM probes.

The AzFPM regioisomers were synthesized from commercially available mannose derivatives and an abundant cellulose degradation product dihydrolevoglucosenone (Cyrene) (Scheme 1B). Reduction of the bicyclic unsaturated compound to an allylic alcohol afforded a compound that could be exploited to yield two diastereomeric epoxides. To generate the 4-azido derivative, we took advantage of halohydrin formation to afford an epoxide that could undergo reaction with azide to ultimately generate compound **9**. In contrast, a nucleophilic epoxidation of the starting material afforded the diastereomeric epoxide that eventually led to the 3-azido analogue. Thus, each route exploited the stereochemical control afforded by the bicyclic precursor to afford the desired derivatives in high yield. In all cases, the critical azide functionality was installed through a nucleophilic displacement or nucleophilic epoxide opening. We appended the (*Z*,*Z*)-farnesyl recognition motif and removed the protecting groups to afford the target compounds (**1**−**4**). The last three steps were rigorously optimized. Their modest yield is due to

https://doi.org/10.1021/jacs.3c09495
J. Am. Chem. Soc. 2024, 146, 377−385

inconsequential counterion speciation and the challenges inherent in the purification of such compounds.

AzFPM Probes Label Mannose-Containing Glycans in Cellulo. We first confirmed that AzFPM probes were incorporated into the cell envelope of model organisms *C. glutamicum* and *M. smegmatis* (Figure 2A). Bacterial cultures

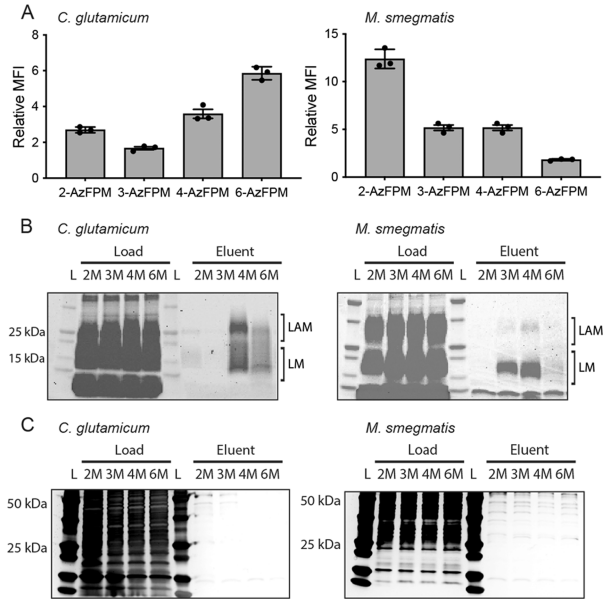

Figure 2. AzFPM labelingin cellulo. (A) Flow cytometry analysis of AzFPM (125 μM)-labeled *C. glutamicum* and *M. smegmatis* treated with DBCO-AF647. MFI was calculated by using the geometric mean and plotted relative to a dye-only control. Error bars denote the standard error of the mean of the three replicate experiments. (B) Streptavidin-enrichment of labeled glycans from AzFPM (125 μM)-labeled *C. glutamicum* and *M. smegmatis* reacted with DBCO-biotin. Load and eluent analyzed by SDS-PAGE using the Pro-Q Emerald 300 glycan staining kit. (C) Streptavidin-enrichment of labeled proteins from AzFPM (125 μM)-labeled *C. glutamicum* and *M. smegmatis* reacted with DBCO-biotin. Load and eluent analyzed by SDS-PAGE using silver stain. L: ladder, 2M: 2-AzFPM, 3M: 3-AzFPM, 4M: 4-AzFPM, 6M: 6-AzFPM. Data are representative of two independent experiments.

were supplemented with AzFPM in media and grown to the late-logarithmic phase. Probes at this concentration did not affect cell viability, though at higher concentrations 2-AzFPM inhibited growth in *M. smegmatis* (Figure SI-1). Following growth, the labeled cells were washed to remove any remaining free probe and then exposed to Alexa Fluor 647 (AF647)-conjugated dibenzocyclooctyne (DBCO). Thus, the fluorescent label was appended via a strain-promoted azide−alkyne cycloaddition (SPAAC).[42] Fixed samples were analyzed by flow cytometry (Figure SI-2).

AzFPM-treated cells had increased fluorescence relative to cells treated only with the DBCO-dye conjugate. The degree of AzFPM incorporation, measured by flow-cytometry-derived relative mean fluorescence intensity (MFI) levels, varied across organisms. In *M. smegmatis*, the 2-AzFPM probe was efficiently utilized, whereas the incorporation of the 6-AzFPM probe was negligible. In *C. glutamicum*, the 6-AzFPM probe afforded the highest levels of incorporation, whereas the signal from the 3-AzFPM probe was minor. The labeling was dose-dependent (Figure SI-3). These findings indicate that the AzFPM probes are substrates for mycobacterial mannosyltransferases. The organism-dependent labeling of each regioisomer highlights the value of testing different isomers. Moreover, the results could not have been predicted solely from the propensity of different probes to result in chain termination. We validated that the observed flow cytometry data correlated with membrane-localized labeling using super-resolution structured illumination microscopy (SIM) (Figure SI-4). These results demonstrate the generality of biosynthetic incorporation probes bearing farnesyl lipid motifs.

We then isolated the labeled structures to assess the specificity of our strategy. Cells grown in media supplemented with AzFPM were then labeled for enrichment by reaction with DBCO-biotin. To capture the modified components, the cells were lysed, and beads modified with streptavidin were added. The bead-captured compounds were analyzed by gel electrophoresis using a glycan stain. We detected bands consistent with the expected molecular weight for LAM and LM (Figure 2B). In *C. glutamicum*, 4- and 6-AzFPM primarily label the LAM. In *M. smegmatis*, the 3- and 4-AzFPM result in robust LM labeling with some signal from the LAM. Although the LAM contains arabinose residues in addition to mannose residues, the AzFPA probes were not incorporated into the LAM but only into the arabinogalactan (Figure SI-5). This selectivity is unexpected as the arabinofuranose polymers in the LAM and the arabinogalactan are thought to be biosynthesized by the same enzymes using an identical lipid-linked donor.[43−47] Our probes indicate differences in the biosynthesis of these two cell envelope components that suggest further investigations are needed.

To investigate AzFPM-labeling selectivity, we visualized the enriched samples using silver stain, given its high sensitivity relative to conventional Coomassie stains.[48] No enriched soluble proteins were detected (Figures 2C, SI-6 and SI-7). This observation indicates that our probes are processed by mannosyltransferases responsible for glycolipid biosynthesis. This result is notable as there is a known mycobacterial membrane-associated protein-*O*-mannosyltransferase (Msmeg_5447) with sequence homology to eukaryotic protein-*O*-mannosyltransferases which accept polyprenyl lipid carrier substrates (dolichol-phosphate). Thus, despite the similarity in these proposed biosynthetic precursors, AzFPM probes retain specificity for the desired glycolipid targets.

Azide Regioisomer Dictates the Selectivity of PIM Labeling. Although 2-AzFPM is incorporated into *M. smegmatis*, it does not appear to label LAM or LM. Specifically, we could not detect probe incorporation into the LAM or LM. We, therefore, hypothesized that this probe is labeling another mannose-containing structure—PIMs. PIMs are implicated as key virulence factors and are known ligands for C-type lectin dendritic cell (DC)-specific intercellular adhesion molecule 3-grabbing nonintegrin (DC-SIGN).[49] We postulated that 2-AzFPM might be used in the final steps of PIM biosynthesis. To test this possibility, we acquired an *M. smegmatis* deletion lacking the lipid-dependent glycosyltransferase PimE (Figure 3A). This enzyme acts at the first step in which extended PIM and LM/LAM biosynthesis diverge.[50] If 2-AzFPM is labeling PIMs, the knockout cell line should exhibit a decrease in cellular staining.

We observed a stark decrease in staining with 2-AzFPM in *M. smegmatis* ΔpimE compared to wild-type cells. In contrast, we observed only a minor decrease in staining with 3-AzFPM (Figure 3B). We employed 7-hydroxycoumarin-3-carboxylic acid-3-amino-D-alanine (HADA), a fluorescent D-amino acid

https://doi.org/10.1021/jacs.3c09495
J. Am. Chem. Soc. 2024, 146, 377−385

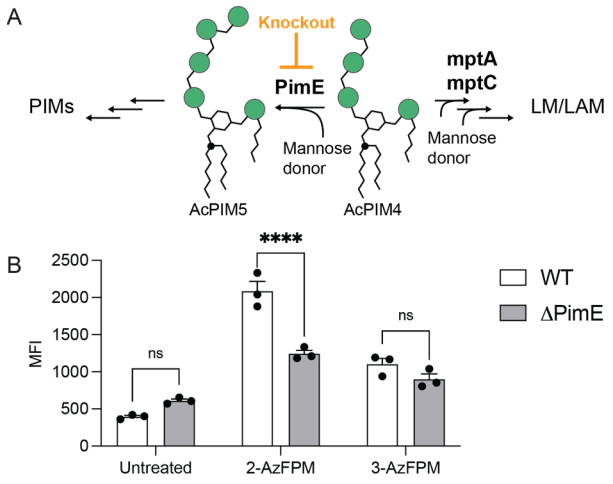

Figure 3. Investigation of PIM labeling using a genetic model. (A) Point of divergence in the biosynthesis of PIMs versus LM and LM indicates the relevance of the PimE knockout. (B) MFI from flow cytometry analysis of AzFPM (125 μM)-labeled *M. smegmatis* wild-type and ΔPimE cells treated with DBCO-AF647. An asterisk denotes a statistically significant differences by two-way ANOVA between samples (****$p < 0.0001$).

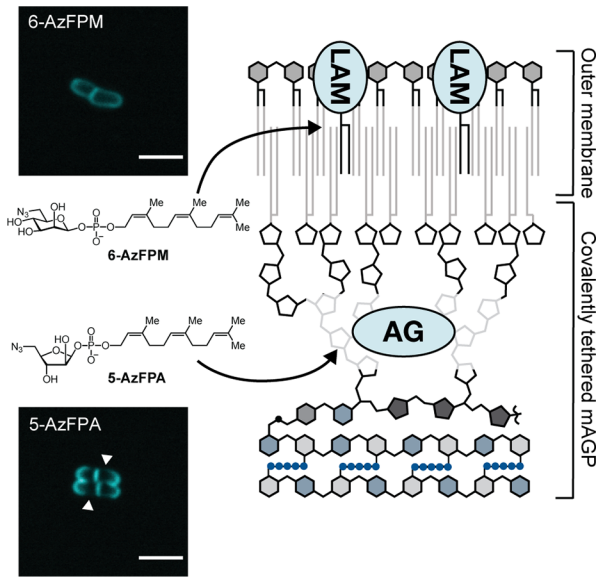

Figure 4. Analysis of localization of AzFPM and AzFPA probes visualized via confocal fluorescence microscopy. Diagram of cell envelope components that are labeled by each probe. Arabinogalactan (AG) is covalently connected to the peptidoglycan, whereas LAM structures are noncovalently embedded in the mycolic acid (MA) layer. mAGP: mycolyl-arabinogalactan-peptidogalactan, PM: plasma membrane. Images taken after a 2 h labeling period (scale bar = 3 μm).

probe that labels the peptidoglycan,[51] to benchmark the decrease in staining detected in the *M. smegmatis* ΔpimE cells. A similar degree of staining by HADA was detected in *M. smegmatis* ΔpimE and wild-type cells, demonstrating the metabolic competence of this cell line (Figure SI-8). *C. glutamicum* lacks extended PIMs or a PimE ortholog. As expected, there was no discrepancy between staining and LAM/LM pulldown upon 2-AzFPM exposure in this organism.[28,30] Thus, using a specific azide-substituted mannose isomer, we obtained highly selective labeling of PIMs in wild-type *M. smegmatis*. This finding emphasizes further the utility of biosynthetic incorporation probes for selective labeling of specific glycans.

Visualizing the In Cellulo Biosynthesis of Mannose-Containing Glycans. We next applied these tools to investigate the sites of mannose-containing glycan biosynthesis in cellulo. Peptidoglycan, arabinogalactan, and mycolic acid biosynthesis all occur at the poles and septa of dividing cells. Limited information is available on the sites of LM and LAM biosynthesis or localization. To address this knowledge gap, we labeled *C. glutamicum* with the probe that stained to the greatest extent, 6-AzFPM, and visualized the sites of its localization (Figures 4 and SI-9). We used an incubation time to capture the initial sites of modification and opted for *C. glutamicum* as our model as its brighter staining and larger cell width enable visualization of staining patterns more readily. We compared our results to those obtained with our previously described 5-AzFPA probe as a control for known biosynthesis patterns. Although 5-AzFPA- labeled arabinose localized to the bacterial septa and poles at short time points, 6-AzFPM labeling occurred along the entire cell wall (see Figure SI-10 for quantification). This annular staining suggests that the localization of mannose-containing glycans is decoupled from known areas of cell envelope biosynthesis.

To assess whether this localization corresponds to that of relevant biosynthetic enzymes, we generated C-terminal mCherry fusions of two *M. smegmatis* mannosyltransferases, one which forms α-1,6 linkages, mptA (Msmeg_4241), and the other which forms α-1,2 branching linkages mptC (Msmeg_4247) (Figure SI-11). We performed these experiments in *M. smegmatis* as this model has a more elaborated LAM structure. The fluorescent proteins localized primarily at the septa rather than displaying homogeneous fluorescence along the entire cell wall (Figure SI-12). The decoupling of the localization between the labeled mannose-containing glycans and biosynthetic enzymes suggests that the mannosylated glycolipids freely diffuse.

Tracking Diffusion of Mannose-Containing Glycans. While the inner mycolate and arabinogalactan are covalently linked to the peptidoglycan, the PIMs, LM, and LAM are noncovalently embedded in the outer and inner lipid membranes. Our observations that the localization of the labeled glycolipids and the biosynthetic enzymes are decoupled indicate that the LM and LAM can rapidly diffuse throughout the cell membrane. We tested this hypothesis by employing our chemical probes in fluorescence recovery after photobleaching (FRAP). In FRAP, a portion of the labeled cell is photobleached, and the cell is visualized over a recovery period. If the fluorophore is attached to a diffusible entity, the surrounding fluorescent molecules will redistribute over the bleached spot to restore its signal. If the labeled structure is covalently tethered, it will not diffuse and the photobleached region will remain dark.

We performed FRAP in both *C. glutamicum* and *M. smegmatis* after AzFPM treatment and labeling. The results were compared to those obtained with AzFPA,[37] which our data indicated led to covalent labeling of the arabinogalactan (Figure 5). As anticipated, cells treated with AzFPA and labeled with a fluorophore did not recover fluorescence after photobleaching. In contrast, cells with modified mannosylated glycolipids afforded a fluorescence recovery. Moreover, FRAP experiments revealed that the rate of diffusion varied among model organisms. Those with longer mycolic acids (e.g., *M.*

https://doi.org/10.1021/jacs.3c09495
J. Am. Chem. Soc. 2024, 146, 377−385

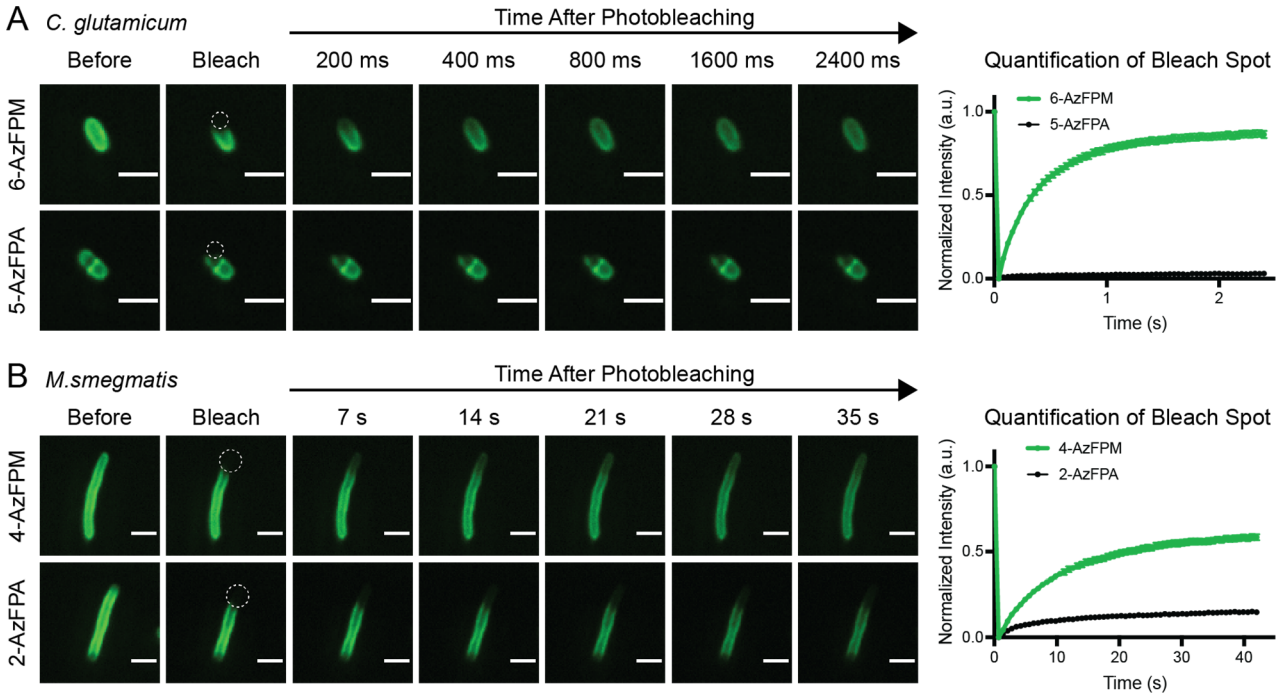

Figure 5. FRAP analysis to track glycan diffusion. Representative FRAP profiles of FPM- or FPA-treated *C. glutamicum* (A) or *M. smegmatis* cells (B). White dashed circles indicate the areas of photobleaching (scale bar = 3 μm). On the right, fluorescence recovery traces for the cells are shown. Error bars denote the standard error of the mean (n = 50 cells).

smegmatis versus *C. glutamicum*) led to slower diffusion. This trend is consistent with previous studies employing mycolate probes.[52] To provide another test that could distinguish the movement of mannosylated lipids versus proteins, we employed formaldehyde fixation. Formaldehyde reacts with available amines, thereby immobilizing proteins. If our probes yielded mannosylated proteins, they would preserve the photobleached area. In contrast, formaldehyde treatment had no effect on fluorescence recovery, indicating that the mannosylated structures retain the ability to diffuse (Figure SI-13). These data are consistent with glycolipid rather than glycoprotein labeling. These findings provide a first glimpse of LAM or LM diffusion on the mycobacterial cell surface (Figure SI-14). Similar experiments using 2-AzFPM to label PIMs in *M. smegmatis* indicated that the PIMs also readily diffuse (Figure SI-15). The rates of PIMs, LM, and LAM diffusion in *M. smegmatis* were similar. Thus, the organisms' cell wall structure and lipid anchor dictate the rate of diffusion.

Testing FPM Probes in Mtb. Though much informative mycobacterial research is derived from nonpathogenic species within the genus,[53] the importance of the LAM for disease led us to assess the utility of the probes in *Mtb*. Thus, we evaluated incorporation by flow cytometry (Figure 6A). The level of incorporation for different probe regioisomers in *Mtb* was similar to that seen in *M. smegmatis* (Figure SI-16). We next enriched the labeled structures by modifying them with DBCO-biotin and performing streptavidin pull-downs (Figure 6B). As with *M. smegmatis*, *Mtb* exposed to 2-AzFPM afforded bright staining, but we detected no probe incorporation into the LAM or LM. In contrast, 3-AzFPM and 4-AzFPM robustly labeled both the LAM and LM. Thus, as in *M. smegmatis*, 2-AzFPM likely labels the PIMs in *Mtb*. Finally, we treated cells with 3-AzFPM and appended a fluorophore, which labels the LAM and LM (Figure 6C). We observed annular staining with the brightest staining at the poles and septum. Together, our

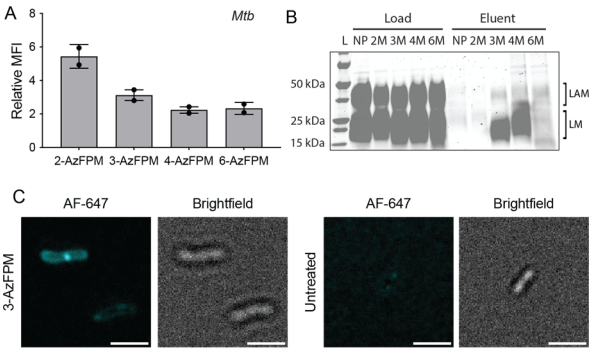

Figure 6. AzFPM labeling in *Mtb*. (A) Flow cytometry analysis of AzFPM (125 μM)-labeled *Mtb* treated with DBCO-AF647. MFI was calculated using the geometric mean and plotted relative to a dye-only control. Error bars denote the standard error of the mean of two replicate experiments. (B) Streptavidin-enriched labeled structures from AzFPM (125 μM)-labeled *Mtb* reacted with DBCO-biotin. Load and eluent analyzed by SDS-PAGE using a Pro-Q Emerald 300 glycan staining kit. (C) Confocal fluorescence microscopy images of *Mtb* grown with 3-AzFPA (125 μM) (scale bar = 3 μm). Abbreviations: L = ladder; NP = no probe; M: 2-AzFPM, 3M: 3-AzFPM, 4M: 4-AzFPM, 6M: 6-AzFPM.

data highlight the versatility of these probes in different mycolic acid-containing species. We anticipate that these new tools will provide further insight into the role of mannose-containing glycans in pathogenic mycobacteria.

CONCLUSIONS

We generated a suite of biosynthetic incorporation probes and showed that they can be used to visualize mannose-containing glycans in mycobacteria. These probes can reveal the location of the PIMs, LM, or LAM on the cell surfaces of wild-type mycobacteria. Using late-stage biosynthetic intermediates, we

https://doi.org/10.1021/jacs.3c09495
J. Am. Chem. Soc. 2024, 146, 377−385

could specifically target immunomodulatory structures on mycobacteria's cell surface without engaging the biochemical pathways involved in mannose metabolism. We observed that the structures labeled are dictated by the regioisomeric donor employed and that specific donors allow the selective labeling of specific glycans (e.g., PIMs versus other mannosylated lipids). We used these features to track the diffusion of specific glycans on the cell surface. Our findings highlight the utility of a farnesyl-based scaffold to mimic lipids beyond a decaprenyl donor, including the polyprenyl donor used for mannose biosynthesis. Members of the targeted GT-C class of glycosyltransferases are found in humans, yeast, archaea, and bacteria. Thus, these glycolipid donor surrogates could install labels onto a wide range of future glycan targets, making these previously invisible cellular components visible.

■ ASSOCIATED CONTENT

Supporting Information

The Supporting Information is available free of charge at https://pubs.acs.org/doi/10.1021/jacs.3c09495.

Experimental procedures, characterization data, probe viability determined by Alamar Blue assay, flow cytometry scatter plots, dose dependence of staining, SDS-PAGE analysis, Western blots, confocal microscopy, heat maps, flow cytometry histograms, fluorescence microscopy, quantification of fluorescence recovery, and synthesis of AzFPM regioisomers (PDF)

■ AUTHOR INFORMATION

Corresponding Author

Laura L. Kiessling − *Department of Chemistry, Massachusetts Institute of Technology, Cambridge, Massachusetts 02139, United States; Department of Chemistry, University of Wisconsin Madison, Madison, Wisconsin 53706, United States; Ragon Institute of MGH, MIT, and Harvard, Cambridge, Massachusetts 02139, United States;* orcid.org/0000-0001-6829-1500; Email: kiesslin@mit.edu

Authors

So Young Lee − *Department of Chemistry, Massachusetts Institute of Technology, Cambridge, Massachusetts 02139, United States;* orcid.org/0009-0003-2026-496X

Victoria M. Marando − *Department of Chemistry, Massachusetts Institute of Technology, Cambridge, Massachusetts 02139, United States;* orcid.org/0000-0002-3557-5838

Stephanie R. Smelyansky − *Department of Chemistry, Massachusetts Institute of Technology, Cambridge, Massachusetts 02139, United States;* orcid.org/0009-0004-2930-2907

Daria E. Kim − *Department of Chemistry, Massachusetts Institute of Technology, Cambridge, Massachusetts 02139, United States;* orcid.org/0000-0001-5711-7929

Phillip J. Calabretta − *Department of Chemistry, Massachusetts Institute of Technology, Cambridge, Massachusetts 02139, United States; Department of Chemistry, University of Wisconsin Madison, Madison, Wisconsin 53706, United States*

Theodore C. Warner − *Department of Chemistry, Massachusetts Institute of Technology, Cambridge, Massachusetts 02139, United States;* orcid.org/0000-0001-7402-0424

Bryan D. Bryson − *Department of Biological Engineering, Massachusetts Institute of Technology, Cambridge, Massachusetts 02139, United States; Ragon Institute of MGH, MIT, and Harvard, Cambridge, Massachusetts 02139, United States*

Complete contact information is available at: https://pubs.acs.org/10.1021/jacs.3c09495

Author Contributions

⊥S.Y.L. and V.M.M. contributed equally.

Author Contributions

The manuscript was written through the contributions of all authors. All authors approved the final version of the manuscript.

Funding

This research was supported by the National Institute of Allergy and Infectious Disease (R01 Al-126592 to L.L.K.), the NIH Common Fund (U01GM125288 to L.L.K.), the NIH (R01A1022553 and R01AR073252 to B.D.B.), NIH-NIGMS (F32 GM142288 to D.E.K.), NSF-GRFP (GRFP 2141064 to T.C.W. and GRFP 1745302 and 2141064 to S.R.S.), and the NSERC (PGSD Fellowship for V.M.M.) for financial support. This work was performed in part in the Ragon Institute BSL3 core, which is supported by the NIH-funded Harvard University Center for AIDS Research (P30 AI060354).

Notes

The authors declare no competing financial interest.

■ ACKNOWLEDGMENTS

M. smegmatis ΔpimE was generously provided by the Morita Group (UMass Amherst). The authors thank V. Lensch and A. Gabba for their assistance in reviewing the manuscript and H. L. Hodges and R. L. McPherson for helpful scientific discussions. The authors also thank Jeffrey R. Kuhn of the Microscopy Core Facility at the Koch Institute Robert A. Swanson Biotechnology Center for technical support with super-resolution microscopy. They thank the WM Keck imaging facility at the Whitehead Institute for ANDOR confocal microscopy. Compound characterization was performed at the MIT Department of Chemistry Instrumentation Facility.

■ REFERENCES

(1) Chakaya, J.; Petersen, E.; Nantanda, R.; Mungai, B. N.; Migliori, G. B.; Amanullah, F.; Lungu, P.; Ntoumi, F.; Kumarasamy, N.; Maeurer, M.; et al. The WHO Global Tuberculosis 2021 Report - Not So Good News and Turning the Tide Back to End TB. *Int. J. Infect Dis* **2022**, *124*, S26−S29.

(2) Ding, C.; Hu, M.; Guo, W.; Hu, W.; Li, X.; Wang, S.; Shangguan, Y.; Zhang, Y.; Yang, S.; Xu, K. Prevalence Trends of Latent Tuberculosis Infection at the Global, Regional, and Country Levels from 1990−2019. *Int. J. Infect Dis* **2022**, *122*, 46−62.

(3) Chandra, P.; Grigsby, S. J.; Philips, J. A. Immune Evasion and Provocation by Mycobacterium tuberculosis. *Nat. Rev. Microbiol* **2022**, *20* (12), 750−766.

(4) Mir, M. A.; Mir, B.; Kumawat, M.; Alkhanani, M.; Jan, U. Manipulation and Exploitation of Host Immune System by Pathogenic Mycobacterium tuberculosis for its Advantage. *Future Microbiol* **2022**, *17*, 1171−1198.

(5) Kumar, A.; Shivangi; Agarwal, P.; S. Meena, L. Interconnection of Mycobacterium tuberculosis With Host Immune System. *J. Respir. Dis. Med.* **2020**, *2* (2), 1−6.
(6) Flynn, J. L.; Chan, J. Immune Evasion by Mycobacterium tuberculosis: Living With the Enemy. *Curr. Opin Immunol* **2003**, *15* (4), 450−455.
(7) Liu, C. F.; Tonini, L.; Malaga, W.; Beau, M.; Stella, A.; Bouyssie, D.; Jackson, M. C.; Nigou, J.; Puzo, G.; Guilhot, C.; et al. Bacterial Protein-O-Mannosylating Enzyme is Crucial for Virulence of Mycobacterium tuberculosis. *Proc. Natl. Acad. Sci. U. S. A.* **2013**, *110* (16), 6560−6565.
(8) Zhou, K. L.; Li, X.; Zhang, X. L.; Pan, Q. Mycobacterial Mannose-Capped Lipoarabinomannan: a Modulator Bridging Innate and Adaptive Immunity. *Emerg Microbes Infect* **2019**, *8* (1), 1168−1177.
(9) Briken, V.; Porcelli, S. A.; Besra, G. S.; Kremer, L. Mycobacterial Lipoarabinomannan and related Lipoglycans: From Biogenesis to Modulation of the Immune Response. *Mol. Microbiol.* **2004**, *53* (2), 391−403.
(10) Barnes, P. F.; Chatterjee, D.; Abrams, J. S.; Lu, S.; Wang, E.; Yamamura, M.; Brennan, P. J.; Modlin, R. L. Cytokine Production Induced by Mycobacterium tuberculosis Lipoarabinomannan. *J. Immunol.* **1992**, *149* (2), 541−547.
(11) Torrelles, J. B.; Schlesinger, L. S. Diversity in Mycobacterium tuberculosis Mannosylated Cell Wall Determinants Impacts Adaptation to the Host. *Tuberculosis (Edinb)* **2010**, *90* (2), 84−93.
(12) Ishikawa, E.; Mori, D.; Yamasaki, S. Recognition of Mycobacterial Lipids by Immune Receptors. *Trends Immunol* **2017**, *38* (1), 66−76.
(13) Fukuda, T.; Matsumura, T.; Ato, M.; Hamasaki, M.; Nishiuchi, Y.; Murakami, Y.; Maeda, Y.; Yoshimori, T.; Matsumoto, S.; Kobayashi, K.; et al. Critical roles for lipomannan and lipoarabinomannan in cell wall integrity of mycobacteria and pathogenesis of tuberculosis. *mBio* **2013**, *4* (1), e00472−00412.
(14) Hayakawa, E.; Tokumasu, F.; Nardone, G. A.; Jin, A. J.; Hackley, V. A.; Dvorak, J. A. A Mycobacterium tuberculosis-derived Lipid Inhibits Membrane Fusion by Modulating Lipid Membrane Domains. *Biophys. J.* **2007**, *93* (11), 4018−4030.
(15) Choudhary, A.; Patel, D.; Honnen, W.; Lai, Z.; Prattipati, R. S.; Zheng, R. B.; Hsueh, Y. C.; Gennaro, M. L.; Lardizabal, A.; Restrepo, B. I.; et al. Characterization of the Antigenic Heterogeneity of Lipoarabinomannan, the Major Surface Glycolipid of Mycobacterium tuberculosis, and Complexity of Antibody Specificities toward This Antigen. *J. Immunol.* **2018**, *200* (9), 3053−3066.
(16) Corrigan, D. T.; Ishida, E.; Chatterjee, D.; Lowary, T. L.; Achkar, J. M. Monoclonal antibodies to lipoarabinomannan/arabinomannan – characteristics and implications for tuberculosis research and diagnostics. *Trends Microbiol.* **2023**, *31* (1), 22−35.
(17) Kaur, D.; Lowary, T. L.; Vissa, V. D.; Crick, D. C.; Brennan, P. J. Characterization of the Epitope of Anti-Lipoarabinomannan Antibodies as the Terminal Hexaarabinofuranosyl Motif of Mycobacterial Arabinans. *Microbiology* **2002**, *148*, 3049−3057.
(18) Nakayama, H.; Oshima, E.; Hotta, T.; Hanafusa, K.; Nakamura, K.; Yokoyama, N.; Ogawa, H.; Takamori, K.; Iwabuchi, K. Identification of Anti-Lipoarabinomannan Antibodies Against Mannan Core and Their Effects on Phagocytosis of Mycobacteria by Human Neutrophils. *Tuberculosis* **2022**, *132*, No. 102165.
(19) Torrelles, J. B.; Chatterjee, D. Collected Thoughts on Mycobacterial Lipoarabinomannan, a Cell Envelope Lipoglycan. *Pathogens* **2023**, *12*, 11.
(20) Bertozzi, C. R.; Kiessling, L. L. Chemical Glycobiology. *Science* **2001**, *291*, 2357−2364.
(21) Andolina, G.; Wei, R.; Liu, H.; Zhang, Q.; Yang, X.; Cao, H.; Chen, S.; Yan, A.; Li, X. D.; Li, X. Metabolic Labeling of Pseudaminic Acid-Containing Glycans on Bacterial Surfaces. *ACS Chem. Biol.* **2018**, *13* (10), 3030−3037.
(22) Barrett, K.; Dube, D. H. Chemical Tools to Study Bacterial Glycans: A Tale from Discovery of Glycoproteins to Disruption of Their Function. *Isr. J. Chem.* **2023**, *63*, No. e202200050.
(23) Dube, D. H.; Bertozzi, C. R. Metabolic Oligosaccharide Engineering as a Tool for Glycobiology. *Curr. Opin Chem. Biol.* **2003**, *7* (5), 616−625.
(24) Liang, H.; DeMeester, K. E.; Hou, C. W.; Parent, M. A.; Caplan, J. L.; Grimes, C. L. Metabolic Labelling of the Carbohydrate Core in Bacterial Peptidoglycan and its Applications. *Nat. Commun.* **2017**, *8* (1), 15015.
(25) Zheng, Q.; Chang, P. V. Shedding Light on Bacterial Physiology with Click Chemistry. *Isr. J. Chem.* **2023**, *63*, No. e202200064.
(26) Gilormini, P. A.; Batt, A. R.; Pratt, M. R.; Biot, C. Asking More from Metabolic Oligosaccharide Engineering. *Chem. Sci.* **2018**, *9* (39), 7585−7595.
(27) Banahene, N.; Kavunja, H. W.; Swarts, B. M. Chemical Reporters for Bacterial Glycans: Development and Applications. *Chem. Rev.* **2022**, *122* (3), 3336−3413.
(28) Cashmore, T. J.; Klatt, S.; Yamaryo-Botte, Y.; Brammananth, R.; Rainczuk, A. K.; McConville, M. J.; Crellin, P. K.; Coppel, R. L. Identification of a Membrane Protein Required for Lipomannan Maturation and Lipoarabinomannan Synthesis in Corynebacterineae. *J. Biol. Chem.* **2017**, *292* (12), 4976−4986.
(29) Nilsson, I.; Grove, K.; Dovala, D.; Uehara, T.; Lapointe, G.; Six, D. A. Molecular Characterization and Verification of azido-3,8-dideoxy-d-manno-oct-2-ulosonic acid Incorporation into Bacterial Lipopolysaccharide. *J. Biol. Chem.* **2017**, *292* (48), 19840−19848.
(30) Rainczuk, A. K.; Yamaryo-Botte, Y.; Brammananth, R.; Stinear, T. P.; Seemann, T.; Coppel, R. L.; McConville, M. J.; Crellin, P. K. The Lipoprotein LpqW is Essential for the Mannosylation of Periplasmic Glycolipids in Corynebacteria. *J. Biol. Chem.* **2012**, *287* (51), 42726−42738.
(31) Wang, Y.; Li, L.; Yu, J.; Hu, H.; Liu, Z.; Jiang, W.; Xu, W.; Guo, X.; Wang, F.; Sheng, J. Imaging of Escherichia coli K5 and Glycosaminoglycan Precursors via Targeted Metabolic Labeling of Capsular Polysaccharides in Bacteria. *Sci. Adv.* **2023**, *9*, No. ead4770.
(32) Yi, W.; Liu, X.; Li, Y.; Li, J.; Xia, C.; Zhou, G.; Zhang, W.; Zhao, W.; Chen, X.; Wang, P. G. Remodeling Bacterial Polysaccharides by Metabolic Pathway Engineering. *Proc. Natl. Acad. Sci. U. S. A.* **2009**, *106* (11), 4207−4212.
(33) Hodges, H.; Obeng, K.; Avanzi, C.; Ausmus, A. P.; Angala, S. K.; Kalera, K.; Palcekova, Z.; Swarts, B. M.; Jackson, M. Azido Inositol Probes Enable Metabolic Labeling of Inositol-Containing Glycans and Reveal an Inositol Importer in Mycobacteria. *ACS Chem. Biol.* **2023**, *18* (3), 595−604.
(34) Morita, Y. S.; Fukuda, T.; Sena, C. B.; Yamaryo-Botte, Y.; McConville, M. J.; Kinoshita, T. Inositol Lipid Metabolism in Mycobacteria: Biosynthesis and Regulatory Mechanisms. *Biochim. Biophys. Acta* **2011**, *1810* (6), 630−641.
(35) Patterson, J. H.; Waller, R. F.; Jeevarajah, D.; Billman-Jacobe, H.; McConville, M.; J. Mannose Metabolism is Required for Mycobacterial Growth. *Biochem. J.* **2003**, *372*, 77−86.
(36) Lommel, M.; Strahl, S. Protein O-mannosylation: Conserved from bacteria to humans. *Glycobiology* **2009**, *19* (8), 816−828.
(37) Marando, V. M.; Kim, D. E.; Calabretta, P. J.; Kraft, M. B.; Bryson, B. D.; Kiessling, L. L. Biosynthetic Glycan Labeling. *J. Am. Chem. Soc.* **2021**, *143* (40), 16337−16342.
(38) Marando, V. M.; Kim, D. E.; Kiessling, L. L. Biosynthetic Incorporation for Visualizing Bacterial Glycans. *Methods Enzymol* **2022**, *665*, 135−151.
(39) Kaur, D.; Berg, S.; Dinadayala, P.; Gicquel, B.; Chatterjee, D.; McNeil, M. R.; Vissa, V. D.; Crick, D. C.; Jackson, M.; Brennan, P. J. Biosynthesis of Mycobacterial Lipoarabinomannan: Role of a Branching Mannosyltransferase. *Proc. Natl. Acad. Sci. U. S. A.* **2006**, *103* (37), 13664−13669.
(40) Mishra, A. K.; Krumbach, K.; Rittmann, D.; Appelmelk, B.; Pathak, V.; Pathak, A. K.; Nigou, J.; Geurtsen, J.; Eggeling, L.; Besra, G. S. Lipoarabinomannan Biosynthesis in Corynebacterineae: the

https://doi.org/10.1021/jacs.3c09495
J. Am. Chem. Soc. 2024, 146, 377−385

Interplay of Two alpha(1–>2)-mannopyranosyltransferases MptC and MptD in Mannan Branching. *Mol. Microbiol.* **2011**, *80* (5), 1241–1259.
(41) Calabretta, P. J.; Hodges, H. L.; Kraft, M. B.; Marando, V. M.; Kiessling, L. L. Bacterial Cell Wall Modification with a Glycolipid Substrate. *J. Am. Chem. Soc.* **2019**, *141* (23), 9262–9272.
(42) Agard, N. J.; Prescher, J. A.; Bertozzi, C. R. A Strain-Promoted [3 + 2] Azide-Alkyne Cycloaddition for Covalent Modification of Biomolecules in Living Systems. *J. Am. Chem. Soc.* **2004**, *126*, 15046–15047.
(43) Alderwick, L. J.; Harrison, J.; Lloyd, G. S.; Birch, H. L. The Mycobacterial Cell Wall–Peptidoglycan and Arabinogalactan. *Cold Spring Harb Perspect Med.* **2015**, *5* (8), No. a021113.
(44) Lee, R. E.; Brennan, P. J.; Besra, G. S. Mycobacterial arabinan biosynthesis: the use of synthetic arabinoside acceptors in the development of an arabinosyl transfer assay. *Glycobiology* **1997**, *7* (8), 1121–1128.
(45) Xin, Y.; Lee, R. E.; S, S. M.; Khoo, K.; Besra, G. S.; Brennan, P. J.; McNeil, M. Characterization of the in vitro synthesized arabinan of mycobacterial cell walls. *Biochem. Biophys. Acta* **1997**, *1335*, 231–234.
(46) Jankute, M.; Grover, S.; Birch, H. L.; Besra, G. S. Genetics of Mycobacterial Arabinogalactan and Lipoarabinomannan Assembly. *Microbiol. Spectr.* **2014**, *2* (4), No. MGM2-0013-2013.
(47) Wolucka, B. A. Biosynthesis of D-arabinose in mycobacteria - a novel bacterial pathway with implications for antimycobacterial therapy. *FEBS J.* **2008**, *275* (11), 2691–2711.
(48) Welsh, J. A.; Jenkins, L. M.; Kepley, J.; Lyons, G. C.; Moore, D. M.; Traynor, T.; Berzofsky, J. A.; Jones, J. C. High Sensitivity Protein Gel Electrophoresis Label Compatible with Mass-Spectrometry. *Biosensors* **2020**, *10*, 11.
(49) Driessen, N. N.; Ummels, R.; Maaskant, J. J.; Gurcha, S. S.; Besra, G. S.; Ainge, G. D.; Larsen, D. S.; Painter, G. F.; Vandenbroucke-Grauls, C. M.; Geurtsen, J.; et al. Role of Phosphatidylinositol Mannosides in the Interaction between Mycobacteria and DC-SIGN. *Infect. Immun.* **2009**, *77* (10), 4538–4547.
(50) Morita, Y. S.; Sena, C. B.; Waller, R. F.; Kurokawa, K.; Sernee, M. F.; Nakatani, F.; Haites, R. E.; Billman-Jacobe, H.; McConville, M. J.; Maeda, Y.; et al. PimE is a Polyprenol-Phosphate-Mannose-Dependent Mannosyltransferase that Transfers the Fifth Mannose of Phosphatidylinositol Mannoside in Mycobacteria. *J. Biol. Chem.* **2006**, *281* (35), 25143–25155.
(51) Siegrist, M. S.; Whiteside, S.; Jewett, J. C.; Aditham, A.; Cava, F.; Bertozzi, C. R. (D)-Amino Acid Chemical Reporters Reveal Peptidoglycan Dynamics of an Intracellular Pathogen. *ACS Chem. Biol.* **2013**, *8* (3), 500–505.
(52) Rodriguez-Rivera, F. P.; Zhou, X.; Theriot, J. A.; Bertozzi, C. R. Visualization of Mycobacterial Membrane Dynamics in Live Cells. *J. Am. Chem. Soc.* **2017**, *139* (9), 3488–3495.
(53) Sparks, I. L.; Derbyshire, K. M.; Jacobs, W. R., Jr; Morita, Y. S. Mycobacterium smegmatis: The Vanguard of Mycobacterial Research. *J. Bacteriol.* **2023**, *205* (1), No. e0033722.

https://doi.org/10.1021/jacs.3c09495
J. Am. Chem. Soc. 2024, 146, 377–385